IAC-13-E2.1

Residual Air Inflated Systems for CubeSats

RUARIDH CLARK*
Mechanical and Aerospace Engineering, University of Strathclyde, United Kingdom

DR EUR ING MALCOLM MACDONALD†
Advanced Space Concepts Laboratory
Mechanical and Aerospace Engineering, University of Strathclyde, United Kingdom

This paper presents a case for the use of residual air inflated (RAI) structures on CubeSat platforms, focusing on the development of a high altitude, de-orbiting device that utilises this deployment method. Residual air inflation relies on small pockets of air, trapped within a sealed membrane, expanding when the structure is exposed to vacuum. This expansion of trapped air then inflates the membrane. The application of this deployment method for a technology demonstrator, to be flown on a European sounding rocket in March 2014, shall be discussed. The demonstrator is a proposed passive, high altitude, end-of-life, deorbiting system that utilises solar radiation pressure. The development of this device from analysis and design through to construction shall be covered with the particular challenges present on a CubeSat platform discussed. The paper shall conclude by proposing possible applications of CubeSat based RAI structures and deployment mechanisms, focusing on the potential for deployment mechanisms and debris capture structures.

I. ACRONYMS

CGG	Cold Gas Generator
FRODO	Foldable and Reflective system for Omni-altitude De-Orbiting
GPS	Global Positioning System
IMU	Inertial Measuring Unit
JPL	Jet Propulsion Laboratory
PCB	Printed Circuit Board
RAI	Residual Air Inflated
REXUS	Rocket-borne EXperiments for University Students
SAM	Self-inflating Adaptive Membrane
SLS	Spring Loaded Structure
SPG	Stored Pressurised Gas
SPI	Sublimating Powder Inflated
W	Weighting factor

II. INTRODUCTION

This paper shall follow the work done in developing a Residual Air Inflated (RAI) system for use on a CubeSat platform, before expanding to look at promising CubeSat based RAI applications. Residual air inflation relies on small pockets of air, trapped within a sealed membrane, expanding when the structure is exposed to vacuum. This expansion of trapped air then inflates the membrane [1]. The paper shall begin with the development and testing of a technology demonstrator called the Foldable and Reflective system for Omni-altitude De-Orbiting (FRODO), through this work and in comparison with other deployment mechanisms the strengths and weaknesses of the RAI method are revealed.

The concept for a high altitude CubeSat de-orbiting device came from a PhD researcher, Charlotte Bewick, at the University of Strathclyde [2] who proposed a reflective cone design that would de-orbit a CubeSat, in around three years, from altitudes that extend beyond the 2000 km cut off for low Earth orbit (see Figure 1). The concept is to use a large reflective area to capture solar radiation pressure, propelling the spacecraft, and increasing the eccentricity of an initially circular orbit. Once the orbit is suitably eccentric the perigee of the orbit shall be close enough to the Earth that the satellite will be captured by atmospheric drag and the deorbit process shall be completed.

*ruaridh.clark@uni.strath.ac.uk
†malcolm.macdonald.102@strath.ac.uk

Copyright ©2013 by Ruaridh Clark. Published by the IAF, with permission and released to the IAF to publish in all forms.

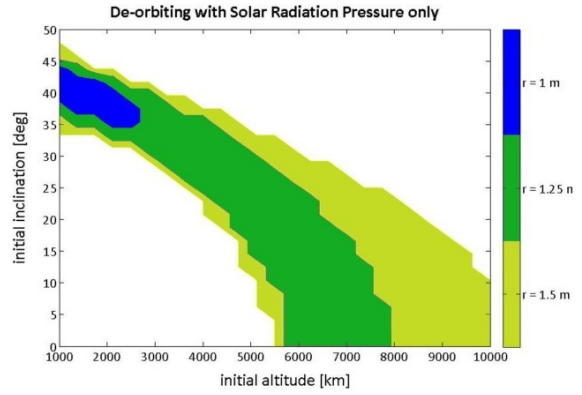

Figure 1: Effective deorbiting regions for cones of different radii with 30° inclination [5]

The 'shuttlecock' effect is proposed to maintain the device in a sun pointing position, with no active control required, as the centre of pressure is displaced from the centre of mass. The only stable position, when the system is statically balanced, is when the centre of pressure is in line with and behind the centre of mass relative to the sun [3].

III. CUBESAT DE-ORBITING DEVICE CONCEPT

This section details the attempts made to realise the FRODO concept and manufacture a testable device for use in a milli-gravity and pressure environment.

III.I. DESIGN SELECTION

The first step taken in designing this CubeSat de-orbiting device was the selection of a suitable deployment mechanism for what is a large structure when considering the size of the CubeSat platform. Utilising the Pugh method for concept selection [4] the following deployment mechanisms were compared; Residual Air Inflated (RAI), Powder Sublimating Powder Inflated (SPI), Stored Pressurised Gas (SPG), Cold Gas Generator (CGG) and Spring Loaded Structure (SLS). A set of selection criteria were created to determine a deployment method, with a focus on feasibility as well as performance. By using a weighting factor (W) in Table 1, ranging from 1 (least important) to 5 (most important) for these selection criterion, each method was rated with a value between 1 (worst) and 5 (best) for each criteria. The RAI and PSI methods proved most suitable, with the RAI method only slightly ahead because of the difficulties in acquiring sublimating powder.

Selection Criteria	W	RAI	SPI	SPG	CGG	SLS
Packaged Volume	**5**	5	5	3	3	2
Reliability	**4**	4	4	3	2	3
Structure Complexity	**3**	5	5	4	4	1
On-ground Testability	**2**	2	2	3	2	4
Ease of Manufacture	**1**	5	4	3	3	1
Total		65	64	48	42	34

Table 1: Deployment mechanism trade-off

Fortunately the RAI and SPI methods are both passive with the structural design not being influenced much by which method was finally selected. Therefore the RAI method was taken forward with SPI as a back-up option if any issues arose during testing.

The next step was to identify a suitable configuration for the device's structure. There were four prominent options; the flat, conical, pyramidal or spherical sail. Similar to Table 1, the packaged volume was the most critical of the selection criteria with the CubeSat platform heavily restricting the volume that could be allocated to the deployable structure.

Selection Criteria	W	Flat	Cone	Pyramid	Sphere
Packaged Volume	**5**	5	4	4	2
Passive Stability	**4**	1	3	3	5
Manufacture Simplicity	**3**	4	3	3	1
Ease of Deployment	**2**	4	2	3	2
Ease of Attachment	**1**	2	4	4	1
Total		51	49	51	38

Table 2: Configuration trade-off

From Table 2 it can be seen that the flat and pyramid sail came out as the most promising options with the cone sail coming a close third. The flat sail would have been

Copyright ©2013 by Ruaridh Clark. Published by the IAF, with permission and released to the IAF to publish in all forms.

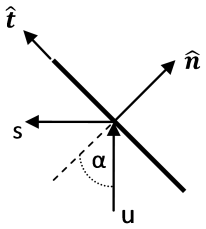

Figure 2: Optical force model.

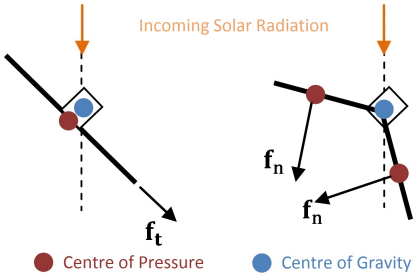

Figure 3: Position of the centre of gravity and pressure for the flat (left) and pyramidal (right) sails.

easier to manufacture, but there were concerns over the passive stability that could be achieved with it. This led to a more in-depth analysis of the passive stability of the flat and pyramidal sails before a final decision would be made on the structural configuration.

III.II. Passive Stability Analysis

A key aspect of the de-orbiting device design is its passive nature. The two most promising sail configurations, flat and pyramidal sail, were analysed with the aim of identifying if the simpler flat sail would provide sufficient passive stability.

The optical force model [6] was used to model the solar radiation acting on the flat surface of the device and can be used to model a sail-fixed two dimensional coordinate frame, $S = \{\hat{n}, \hat{t}\}$, see Figure 2. This model takes into account the optical properties and non-Lambertian nature of the reflecting surface, where the non-Lambertian coefficient details the variation in surface brightness depending on the angle the surface is viewed from.

Optical properties were chosen based on the solar sail designs generated by the Jet Propulsion Laboratory (JPL) [6]. The JPL sail has a highly reflective aluminium coating on the sun facing side and a highly emissive black chromium coating on the shaded side. The reflectivity ($\tilde{r}$), specular reflectivity (s), emissivity (ε) and non-Lambertian coefficient used for the model are detailed in Table 3. It should be noted that these properties will not be accurate for this CubeSat de-orbiting device, however they act as a good first approximation.

$\tilde{r}$	s	ε_f	ε_b	B_f	B_b
0.88	0.05	0.55	0.79	0.55	0.55

Table 3: Solar sail optical properties

In Figure 2 the incoming photons, u, are reflected, s, producing two force vectors, $\hat{n}$ and $\hat{t}$, where the pitch angle, α, is relative to the sun-line. The force vectors are found by summing the force caused by the reflectance, absorption and emissivity of the sail, producing the Equations 1 and 2.

$$\begin{aligned} f_n = PA\big[&(1+s)\cos^2(\alpha) \\ &+ B_f(1-s)\tilde{r}\cos(\alpha) \\ &+ (1-\tilde{r})\Big(\frac{\varepsilon_f B_f - \varepsilon_b B_b}{\varepsilon_f + \varepsilon_b}\Big)\cos(\alpha)\big]\hat{n} \end{aligned} \tag{1}$$

$$f_t = PA[(1+\tilde{r}s)\cos(\alpha)\sin(\alpha)\hat{t} \tag{2}$$

where P is the solar radiation pressure and A the surface area of the sail.

Equations 1 and 2 are then used to find the restoring couple present when the system is displaced from its statically balanced position, represented by Equation 3.

$$\ddot{\theta} = Fd/I \tag{3}$$

where d is the displacement from the centre of mass to the centre of pressure, I is the moment of inertia and F the force perpendicular to the moment arm.

Flat Circular Sail

For the flat circular sail the centre of pressure was assumed to act at the centre of the sail, se Figure 3. The centre of mass for the structure, excluding the sail, is estimated as being 6cm away from the sail since 40% of the volume is assigned to storage of the inflatable. The distance from the centre of mass to the centre of pressure is estimated for this setup to be 5.75 cm. The moment of inertia, I, was found by using Equation 4.

$$I = \Sigma m r^2 \tag{4}$$

Copyright ©2013 by Ruaridh Clark. Published by the IAF, with permission and released to the IAF to publish in all forms.

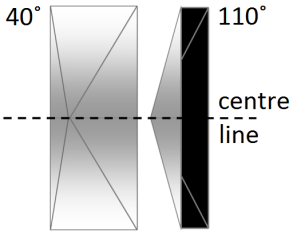

Figure 4: Pyramid sail visible surface areas during rotation

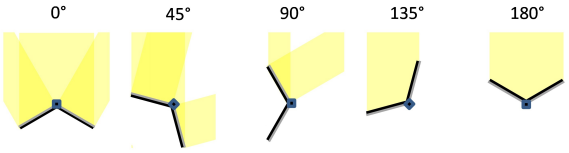

Figure 5: 2D Pyramid sail at pitch angles between 0° and 180°

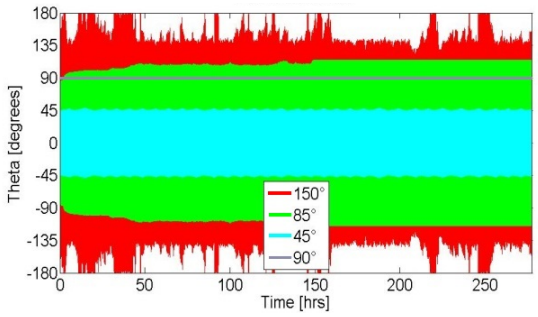

Figure 6: Analysis results for the flat circular sail.

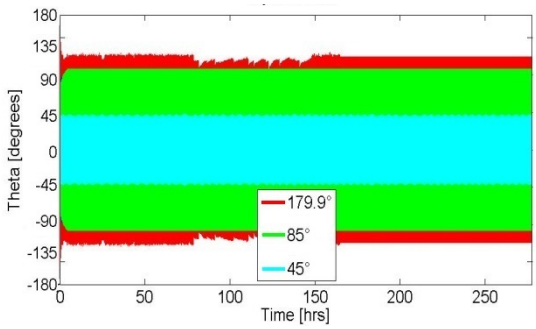

Figure 7: Analysis results for the pyramid sail.

where m is the mass and r is the distance from the centre of mass to the centre of mass of the sail and the CubeSat without the sail.

The component of the solar radiation force equation parallel to the surface, Equation 2, generates the restoring torque for flat sail, as shown in Figure 3.

Pyramid Sail

To simplify the pyramid sail analysis the tip of the pyramid was assumed to be attached to the CubeSat at the centre of mass plus only one oscillation scenario was modelled. This scenario considered only one axis of rotation. The model assuming no roll was present with the plane of oscillation lying on the line of symmetry which cuts two of the triangular surfaces of the pyramid in two, as displayed in Figure 4 where the centre line is the line of symmetry mentioned. These assumptions greatly reduced the model complexity while still being representative of the system for the purposes of comparison with the flat sail. For the purposes of calculating the visible areas, of each section of the pyramid, at any particular angle the equation of each line was determined for a 2D representation of the visible areas as depicted in Figure 4.

The centre of pressure on either side of the pyramid was located by finding the line, parallel to the line at the base, which bisects the area into two areas of equal size. Unlike the flat sail it is the force normal to the surface, Equation 2, which is taken for the two triangular areas either side of the pyramid, as displayed in Figure 3. It is therefore the difference in visible area which produces the restoring couple. The normal force on the other two sides of the pyramid does not influence the oscillations, due to the ideal case assumption, as either side produces an equal but opposing force. However, the parallel force, f_t, cannot be ignored on these side panels. This was approximated by multiplying the parallel force by the cosine of the pitch angle, α, plus or minus 30° depending on which surface was providing the restoring torque. Integration of the line was carried out to determine the visible side area.

By using integration of a line the visible area of the back of the sail not shaded by the pyramid as it turns beyond 90° pitch angle can be found. With the torque distance calculated by finding the line which bisects the exposed area.

Considering the normally shaded (back) side of both of the sails, the coating assumed to be applied here is black chromium used for its high emissivity. This coating also

Copyright ©2013 by Ruaridh Clark. Published by the IAF, with permission and released to the IAF to publish in all forms.

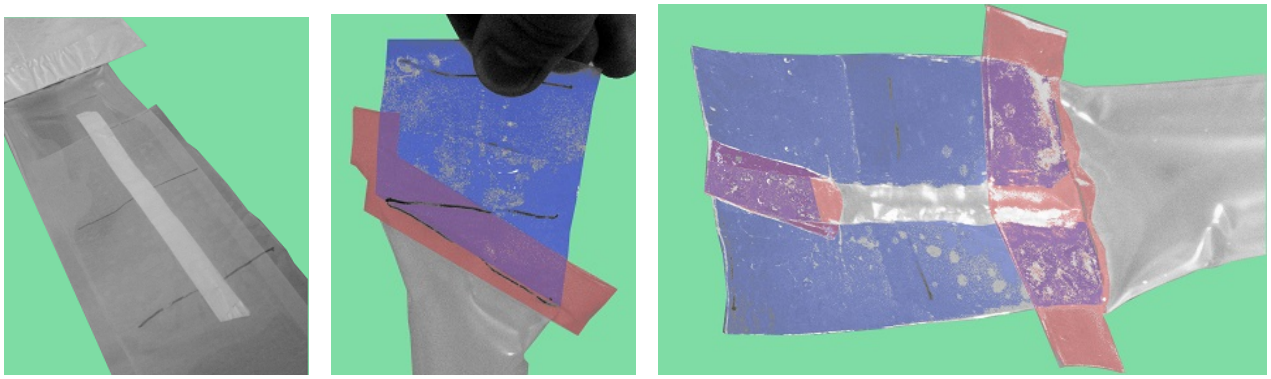

(a) Heat sealing prepared tube (b) Standard seal setup (c) Tube heat sealed with deflating vent

Figure 8: Tube Manufacture images with false colour highlighted areas; heat sealed area (blue) and Tear-aid strip (red).

has a high absorptivity of 0.95. These models shall, therefore, assume the back surface will act like a black body, absorbing all radiation.

The results of this analysis can be seen in Figures 6 and 7 where the model has simulated 'releasing' the sail at a specified angle, monitoring the subsequent oscillations. Figure 6 shows that the flat sail is in an unstable oscillation, when starting from a release angle beyond 150° with the sail never settling and occasionally falling into a spin. Whereas the pyramid with a 30° slope is far more stable and was, therefore, taken forward as the prefered design for manufacture. However it is also evident that for the concept to be successful, with oscillations reducing to near the 0° mark, damping will also have to be incorporated into the structure. Whether this can be achieved through the flexing of the structure or if a separate mechanism is required has not been determined.

III.III. Construction

This section will detail the manufacture of the FRODO test models. The key construction challenge was to achieve a suitably air tight structure for the short duration (∼5 minutes) test flight, discussed in the following section. Difficulties arose with the choice of material for the inflatable booms, polythene, and with a thickness of only 30μm the danger of puncturing the booms was high. Restrictions in facilities and budget meant that the booms were manufactured by hand, using tubing which was cut to length and sealed at either end. The polythene was difficult to work with in this respect as it limited the number of options available for creating an airtight seal.

Residual Air Inflation Tests

Preliminary vacuum tests were used to identify what controls would be required to ensure that the booms would reliably inflate. Therefore two types of boom were constructed; one with little attempt to press the air out of the tubes prior to sealing and the other with weights placed along its length to limit the volume of air within the finished boom.

Testing of these two manufacture processes found that there was little discernible difference in boom inflation with the boom appearing fully inflated and supporting its own weight, for both processes, below 50 mbar. The vacuum chamber used could reach in the region of 0.3 mbar with the test flight pressures expected to be in the region of 0.005 mbar. Thence, the governing factor for the volume of air stored within the booms became the packaging efficiency for the structure; resulting in the booms being as deflated as possible when sealed.

Tube Sealing

In deciding how to seal the ends of the booms the whole structure's assembly and packaging had to be considered. The final structure would have to be first inflated, to ensure that the reflective surface could be attached securely and with sufficient tension to hold it taut, before being fully deflated and resealed. This consideration led to each boom having one sealed end and one end with a sealable vent.

Heat sealing was used to seal the ends of the booms. This technique was ideal for this application as it resulted in a minimal increase in packaging volume for the structure. Unfortunately, the errors incurred by carrying out this process by hand meant that it was not possible to guarantee

Copyright ©2013 by Ruaridh Clark. Published by the IAF, with permission and released to the IAF to publish in all forms.

(a) (b)

Figure 9: Stages of sail attachment

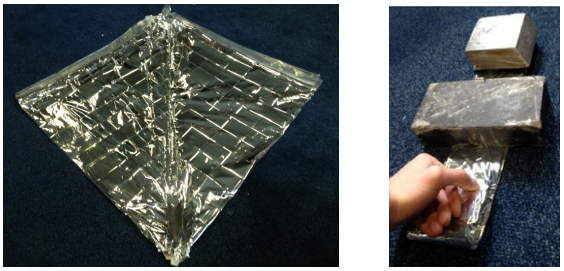

(a) (b)

Figure 10: Stages of sail attachment

a perfect seal every time. Small punctures in the material of the seal, which could release air, were not obvious upon visual inspection and with leaks sometimes only being noted hours after inflation further protective steps were required.

To safeguard against any manufacturing flaws a commercial airtight repair patch, Tear-Aid®, was used along the seal boundary, as shown in Figure 8b and 8c. Figure 8b is of particular note as Tear-aid has also been applied along the left edge of the heat sealed area. This patch has been added due to the formation of an air leak, with the pressurised air forming a channel along the edge of the seal.

The Tear-aid added to the packaged volume but was considered necessary to ensure airtight booms. It should be noted that an attempt to seal the booms using only Tear-aid was made, but the repair patches suffered from leaks and failures when sealing the whole end of the tube.

The final aspect of the boom seal design was the air vent that was required to allow the inflation and deflation of the structure. This was achieved by simply leaving an avenue of unmelted plastic which could be used to insert a pump for boom inflation before being sealed off with a strip of Tear-aid. To deflate the boom again the seal was cut so as to expose the vent and allow the air to leak out. When it came to reseal the boom again heat sealing would be used to close the vent permanently, with another Tear-aid patch required to ensure an airtight seal.

Sail Attachment

To attach the sail to the boom structure double sided adhesive tape was used. Such a solution is unlikely to be suitable for a long duration space mission, but given the budgetary and time constraints it was a suitable solution for the short test flight. The tape was placed along the booms with the structure laid down on the sail material, which was being held taut, as shown in Figure 9a. This process was then repeated for the three other panels with the final finished structure displayed in Figure 9b.

Packaging

Fitting a pyramid structure of $\sim$100 cm^3 within a volume of $\sim$400 cm^3 requires careful planning and folding to ensure that the structure both fits and deploys successfully. Different folding and twisting options were considered for storing the structure, with the constraints being that the peak of the pyramid had to remain exposed so that it could attach to the CubeSat module which would be carrying it for the test flight. Through a trial and error approach it was found that efficient packaging could not be achieved by twisting, with the presence of the booms as well as the pyramid shape responsible for these difficulties. Therefore, all folding options were considered with the aim of both storing the structure effectively and achieving a configuration that would deploy easily. Despite requiring a packaging efficiency of only 25% the inefficiency caused by the booms being attached to the sail material meant a folding configuration was chosen that could be completed by one person and enabled maximum packaging efficiency. The steps undertaken to achieve this packaged structure shall be covered in the following paragraphs.

The structure had to first be laid out with all the booms not making up the square base placed on top of each other. The excess sail material was then laid out with two panels placed on either side of the central booms and folded in the middle of the sail panel, as shown in Figure 10a. Taking one of the edges, where the booms that made up the square base lay, as seen in the top left and right of Figure 10a, and creating a fold with the first fold line lying 8 cm from the aforementioned edge. The structure is then flipped over so that the underside now faces up and

Copyright ©2013 by Ruaridh Clark. Published by the IAF, with permission and released to the IAF to publish in all forms.

(a) (b) (c) (d)

Figure 11: Rapid deployment in vacuum conditions

another 8 cm fold is made. The structure is flipped again and this process is continued until a 9-9.5 cm strip is left. The flipping of the material is necessary as this produces a z-fold which will encourage the unravelling of the structure during deployment. There are many folding patterns available for cylinders that encourage a more stable and controlled inflation [7], but since the sail and cylindrical booms are combined in the one structure an unstable and less controlled deployment has to be accepted.

The final step is to fold the strip of material, as shown in Figure 10b, in 8 cm segments until a block of material approximately 9.5 x 9.5 cm in size remains. Note that the material is folded at 8 cm intervals to achieve the 9.5 cm dimension with the thickness of the sail at this point causing slight expansion with every fold. It can also be seen from Figure 10b that weights were used throughout the folding process to improve packaging efficiency and ease of folding. The folds in this strip were not carried out in a z-fold as it proved too difficult to implement, but in theory this would be a superior folding pattern for encouraging deployment than the roll-like pattern present in this section.

One important issue revealed itself when packaging the second version of the FRODO structure. The main update between the first and second structure versions was the use of tougher tubing that protected better against punctures and damage. The thickness of the tubing used for both versions of the structure was the same, 30 μm, therefore a similar packaged volume was expected. However, the tougher tubing was stiffer which meant that the structure could not be as efficiently folded with the maximum packaging efficiency, originally $\sim 50\%$ for the first version, falling to slightly less than 25% for the second version.

Improvements

There are many areas of improvement for this process when looking forward to manufacturing a space mission worthy device. Bespoke manufacturing of the whole boom would be one obvious improvement, with no further work required to seal off the boom or create a vent. However, without changing the device's construction procedure a seal would have to be created after the final deflation.

Finally, more extensive testing of long term boom inflation as well as the effects of compressed storage while in the space environment is required before the de-orbiting device concept could be verified as feasible.

III.IV. Testing

The preliminary tests for the efficacy of residual air inflation as a method of boom inflation have already been discussed, but further tests were carried out on the full structure. Given the restriction of vacuum chamber volume a limited number of tests could be carried out but the goal of this test campaign was to ensure the RAI structure could be evaluated during the test flight, which is discussed in the following section.

One of the primary concerns to be addressed was the initial deployment of the structure from its confined state within the 100x100x40 mm container. Multiple tests were carried out in which the structure successfully deployed from such a container, but these tests were not representative of the test flight conditions as the structure deployed slowly with the chamber brought from atmospheric pressure to vacuum.

A more representative test was completed by using tensioned wire to hold the inflatable structure within the container until a vacuum of around 0.3 mbar was achieved. At this point a pyrocutter was used to cut the cable and release the lid restraining the structure, as shown in Figure 11. This test showed that the structure successfully deployed and carried on inflating and deploying, however it is still possible that the structure sustained damage from this explosive deployment, as the formation of a small puncture could have occurred which would not be obvious

Copyright ©2013 by Ruaridh Clark. Published by the IAF, with permission and released to the IAF to publish in all forms.

except in the case of a full structure deployment. Such punctures being very difficult to find during visual inspections. Only a full scale test like the one discussed in the following section could satisfactorily prove the survival of the device after rapid deployment.

IV. SOUNDING ROCKET EXPERIMENT

The StrathSat-R experiment was created with the aim of testing the FRODO device, detailed in this paper, and another RAI structure SAM (Self-inflating, Adaptable Membrane)[1]. The experiment secured a launch on a European sounding rocket as one of the European Space Agency (ESA) allocation of payloads on the REXUS programme, which is realised under a bilateral Agency Agreement between the German Aerospace Center (DLR) and the Swedish National Space Board (SNSB).

This sounding rocket launch was chosen as a suitable test for the FRODO device, the rocket apogee of around 85 km providing a space-like environment, with milli-gravity and pressure conditions. The experiment objectives were therefore as follows:

1. Test deployment of the device in milli-gravity and pressure conditions.
2. Test the proposed passive attitude control.
3. Observe the structural integrity of the device during the re-entry as the ambient pressure rises.

Objective 1: Given the size of the FRODO structure, 1.7 m^2 base, there were restrictions on what vacuum tests could be performed on the ground. Even in a suitably large vacuum chamber the deployment of the structure would be restricted and altered due to the strong gravitational influence. In addition to understanding the behaviour of the structure during deployment, the effect of the deployment on the CubeSat's attitude is of interest with minimal disturbance to the CubeSat being desired.

Objective 2: Despite the near-space vacuum conditions present during initial deployment, there is still a notable, rarefied, atmospheric presence. It is envisaged that the 'shuttlecock' passive stability, discussed earlier in the FRODO device's mission concept, can be tested as the structure should point in or oscillate around the direction of its velocity vector. This will almost certainly occur in the denser atmosphere in the latter part of the structure's descent, but it is hoped that evidence of this effect will be present from the onset of the structure's release.

Objective 3: The robustness of the structure shall be tested as it reaches denser atmosphere with the manner of failure being of interest, especially in the case of failure prior to atmospheric pressure rising enough to cause boom deflation.

Figure 12: CubeSat Modules being tested while sitting on experiment housing

IV.I. EXPERIMENT DESIGN

The experiment is housed in a section of the rocket, which has had holes created in it for two hatches and camera viewing windows. The FRODO and SAM inflatable structures are held within two CubeSat-like modules which are ejected out of opposite sides of the rocket. 40% of the CubeSat module volume was assigned to storing the FRODO structure, the rest of the module contains the PCBs, microcontroller, batteries and RF transmitters, with the antennas and parachute attached to the side of the module and covered with a pyrocutter released lid.

The experiment is designed to rely on the pyrocutters actuated by the rocket's service system to release the retention wire that holds the two modules within a set of rails. The modules are to be deployed after the rocket has been de-spun to give the cameras, remaining on-board the rocket, a better opportunity to capture the deployment of the inflatable structures. The ejection of the modules relies upon four compressed springs at the centre of the rails. The deployment of the inflatable structure itself is designed to be completely passive after the initial pyrocutter actuation, to reduce the number of single points of failure. This is achieved by having the hatches held in place

Copyright ©2013 by Ruaridh Clark. Published by the IAF, with permission and released to the IAF to publish in all forms.

by the tensioned retention wire, with these hatches also covering the payload compartment of each module preventing premature deployment of FRODO or SAM. When the main pyrocutters are fired the modules shall be pushed out by the springs while at the same time the inflation of the deployable structures pushes away the hatch lids.

The CubeSat modules themselves record the deployment and descent with an on-board HD camera that sits in the compartment with the PCBs and points out of a viewing hole cut in the side of the module. The camera used is a HackHD, which records 1080p high-definition video to a microSD card. An IMU on-board the module shall be used in conjunction with the recovered footage to determine if the 'shuttlecock' effect was present in the early stages after release.

The data recorded stays with the modules that are recovered by helicopter, after their parachute assisted landing, with GPS coordinates relayed from the module to the ground team by radio signal and through transmission to the Globalstar satellite network.

IV.II. Launch and Lessons Learnt

The StrathSat-R experiment was launched on REXUS 13 in May 2013. Unfortunately a procedure error on the side of Eurolaunch resulted in the cube modules not being ejected. The experiment itself returned intact and shall be relaunched in March 2014 on-board REXUS 15 or 16.

Despite the failed ejection of the modules a couple of important lessons were still taken from this launch campaign.

1. The ingress of hot gases during the rocket's ascent can be damaging to the plastic components of the deployable structures.
   - Kapton film shall be used to protect the structures on the next launch.
2. The stiffer boom material (as mentioned previously) caused difficulties in packaging the structure into the storage container. Therefore the FRODO structure shall need to change, with either a material change or a reduction in size, before the next launch.

V. FUTURE DEVELOPMENT

Although the RAI method has many benefits when used to realise this CubeSat de-orbiting device there are still a number of unknowns and issues that would have to be overcome before it would be considered the ideal choice for such a mission.

A critical unknown is the structure's ability to fully inflate and deploy, if it has been restrained while in vacuum conditions for a prolonged period of time. If sufficient leakage of air, diffusing through the boom material, occurs then RAI would be very restricted in its application and become a high risk deployment option. The limited quantity of stored air resulting in a reduced capacity for coping with any form of leakage.

The risk of gradual deflation is also an important consideration after the RAI structure has deployed. For the de-orbiting mission concept the structure would have to survive years in the space environment, where there is also a risk of micro-meteorite or other debris impact. Hence, it would be necessary to include some form of structure rigidisation to ensure the structure does not collapse or deform. There are a number of options for rigidising inflatable structures, with cold curing resin having been previously proposed as a favourable option for a long term inflatable CubeSat mission [8]. Cold curing resins are typically elastomers that harden when they cool below their glass transition temperature [9].

There are, however, other applications for RAI structures that might face less development obstacles. Some of these more promising applications shall be discussed in the following section.

VI. OTHER RAI STRUCTURE APPLICATIONS

The previous section highlighted the obstacles facing the development of a RAI de-orbiting device but there are other promising CubeSat applications for RAI structures; including deployment mechanisms, to replace traditional spring loaded devices, and also possibly as a debris capture device.

VI.I. Deployment Mechanism

Solar Panel Deployment

The use of residual air inflation is promising as a very low cost and light weight alternative to more complex, spring loaded deployment mechanisms. Given the constraints always present for weight and often for budget, this may be a worthwhile technology to develop for a CubeSat market.

If looking at the potential for solar panel deployment, not only will the aforementioned advantages be present but it opens up the possibility of deploying larger solar arrays than are conventially used with CubeSats. Comparing the potential for RAI deployment with other work on deployment of flexible solar panels, see Figure 13, a RAI solution would require a less bulky mechanism and

Copyright ©2013 by Ruaridh Clark. Published by the IAF, with permission and released to the IAF to publish in all forms.

(a) (b)

Figure 13: Rack and gear, spring loaded, flexible solar panel deployment mechanism.[10]

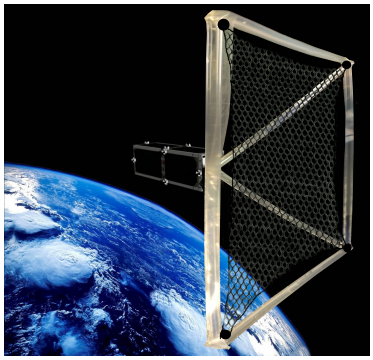

Figure 14: RAI space debris capture concept based on CleanSpace One mission proposal.

have the added advantage of supporting the length of the flexible array.

The concept is to attach a boom along the length of the flexible solar panel and attached to a central rod around which the panel is wrapped in a similar manner to that shown in Figure 13a. A spring is used to push the rod outside of the CubeSat enabling the inflation of the tubing and hence the panel deployment. The one particular advantage that an inflatable solution has in this case is, as mentioned, the support it will provide to the entire length of the array, ensuring that the panels are held in place after deployment. Whereas the solution shown in Figure 13 would risk continued oscillation and disturbance to the solar arrays after the energetic deployment.

VI.II. Debris Capture Device

Looking at more speculative uses of RAI structures, a CubeSat based debris capture system could be feasible. A CubeSat debris capture capability is already being developed by the SwissCube team. The project CleanSpace One [11] plans to capture debris and de-orbit it using a grabbing mechanism and some form of micropropulsion. The difficulty with the proposed grabbing device is that it will require both precise attitude control and debris positional knowledge to capture the debris. Therefore, a RAI structure could reduce the level of positional control required by replacing the small grabbing device with a large net deployed using a RAI frame. One concept for this would be to use a pyramidal configuration with a net held across the square base of the pyramid. Each corner of the net would have a weight attached that is pulled free when the debris impacts upon the net, an artist's impression of such a device is shown in Figure 14. Ensuring that the net deploys without coming loose and that the debris remains trapped and attached to the CubeSat would require carefully design and testing. A preliminary suggestion for entrapping the object would be to use Velcro along the edges of the net which meet and attach when the net collapses after impact with the debris.

VII. CONCLUSION

Residual air inflated structures are certainly in keeping with the CubeSat philosophy of low cost and low mass while accepting higher than convential risks for a space mission. But RAI structures also offer CubeSats the possibility of enhanced capabilities that can achieved with relatively little development time; encouraging bespoke missions by taking away the reliance on complex, expensive and large off-the-shelf spring loaded mechanisms.

The majority of this paper investigated the possibility of utilising the RAI method to deploy a large, pyramidal structure for use as a high altitude, CubeSat, de-orbiting device. Questions remain over this methods suitability for a long term mission with it appearing that a rigidisation option would have to be implemented before such a mission was undertaken.

The first deployment of the FRODO device in milligravity and pressure conditions, after release from the sounding rocket, shall be of great interest not only for the future development of this concept but also for other

Copyright ©2013 by Ruaridh Clark. Published by the IAF, with permission and released to the IAF to publish in all forms.

potential RAI applications. These potential applications were discussed as they take the greatest advantage from the strengths of the RAI method, by providing a cheap, light and simple method of deploying a structure that is larger than its host CubeSat but do not require the long term inflation that may not be achievable with RAI on its own.

VIII. ACKNOWLEDGEMENTS

This work was completed with assistance and guidance from Charlotte Bewick, Thomas Sinn and Daniel García Yárnoz. Thomas McCanny provided valuable assistance in facilitating all vacuum chamber tests. My fellow members of the StrathSat-R team also deserve acknowledgement for their work in developing the sounding rocket experiment. Participation at the International Astronautical Congress 2013 was funded by sponsorship from the British Interplanetary Society (BIS) and the Royal Academy of Engineering (RAEng).

VIII. REFERENCES

[1] Sinn, T., Vasile, M. and Tibert, G., *Design and Development of Deployable Self-inflating Adaptive Membrane.* AIAA-2012-1517, 13th AIAA Gossamer Systems Forum as part of 53rd Structures, Structural Dynamics, and Materials and Co-located Conferences, Honolulu, Hawaii, 23 - 26 April, 2012.

[2] Lücking, C., Colombo, C. & Mcinnes, C., *A passive high altitude deorbiting strategy.* 25th Annual IAA/USU Conference on Small satellites, 2011-08-08 - 2011-08-11, Logan, Utah.

[3] Wie, B., *Solar Sail Attitude Control and Dynamics, Part 1.* Journal of Guidance, Control, and Dynamics, 2004

[4] Pugh, S., *Total Design: Integrated Method for Successful Product Engineering.* Addison Wesley, Wokingham, England, 1991.

[5] Clark, R., Sinn, T., LÃijcking, C., Donaldson, N., Brown, R., Parry, T., Dolan, I., Lowe, C., Bewick, R., âĂIJ StrathSat-R: Deploying Inflatable Cubesat Structures in Micro GravityâĂİ, IAC-12-E2.3.7, 63rd International Astronautical Congress (IAC), Naples, Italy, 1-5 October 2012

[6] McInnes, C., *Solar Sailing Technology, Dynamics and Mission Applications.* Springer, 2004.

[7] *Folding Inflatable Booms.* http://deploytech.eu/science.php [Online], DEPLOYTECH, 2013.

[8] Lücking, C., Colombo, C. and McInnes C. R., *Mission and System Design of a 3U CubeSat for Passive GTO to LEO Transfer.* 63rd International Astronautical Congress, Naples, October, 2012.

[9] Defoort, B., Peypoudat, V., Bernasconi, M. C., Chuda, K. and Coqueret, X., *Recent advances in the Rigidization of Gossamer Structures.* ser. Computational Methods in Applied Sciences, Netherlands: Springer, 2005, vol. 3, pp 259-283.

[10] Tim5989, *Flexible Solar Panel Deployment for Cubesat.* http://www.youtube.com/watch?v=1g45G2z9Ea4 [Online], April, 2012.

[11] Richard, M., Kronig, L., Belloni, F., Rossi, S., Gass, V., Araomi, S., Gavrilovich, I., Shea, H., Paccolat, C. and Thiran, J. P., *Uncooperative Rendezvous and Docking for MicroSats; The case for CleanSpace One.* 6th International Conference on Recent Advances in Space Technologies, RAST 2013, Istambul, Turkey, June, 2013.